jmr&t
Journal of Materials Research and Technology
www.jmrt.com.br

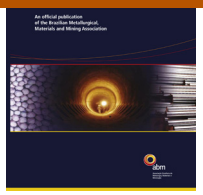

Original Article

Experimental and physical model of the melting zone in the interface of the explosive cladding bar

Bingfeng Wang[a,b,c,*], *Fangyu Xie*[b], *Xiaozhou Luo*[b], *Jindian Zhou*[b]

[a] *State Key Laboratory for Powder Metallurgy, Central South University, Changsha, People's Republic of China*
[b] *School of Materials Science and Engineering, Central South University, Changsha, People's Republic of China*
[c] *Key Lab of Nonferrous Materials, Ministry of Education, Central South University, Changsha, People's Republic of China*

ARTICLE INFO

Article history:
Received 28 August 2015
Accepted 12 April 2016
Available online 24 May 2016

Keywords:
Light microscopy
Composites
Non-ferrous alloys
Welding
Interfaces

ABSTRACT

Local melting zone encountered in sections of the cladding interface is a distinguished phenomenon of the explosive cladding technique. The thickness and morphology of the melting zone in the Ti/NiCr explosive cladding bar are investigated by means of optical microscopy. Results show that the distribution of the melting zone in the interface of the Ti/NiCr explosive cladding bar is uniform and axisymmetric, and boundaries of the melting zone are circular arcs, whose center points to the center of the NiCr bar. The bamboo-shaped cracks generate in the melting zone. The thickness of the melting zone decreases with reducing of the stand-off distance and the thickness of the explosive. A physical model of the melting zone in the interface of the explosive cladding bar is proposed.

1. Introduction

Explosive cladding is a solid state metal joining process which produces a weld joint by high velocity colliding, aided by controlled detonation with an explosive charge [1]. It is best known for its capability to join a wide variety of both similar and dissimilar combinations of metals that cannot be joined by fusion welding or any other bonding methods [2]. Up to now, over 260 various similar and dissimilar metal and alloy combinations can be welded by using explosive cladding technique [3].

Local melting zones, which seriously affect the properties of the explosive cladding composite, are often encountered in sections of the cladding interface. The melting zones showed unique and interesting microstructure and properties become the hot topic of the explosive cladding technique in recent years. The bonding interface of the explosive cladding presents three morphologies: wavy, straight and melting zone [2]. Many scholars have involved themselves into the study of these morphologies. Some researches proposed that the bonding interface changed from a straight to a wavy structure with increasing the explosive loading and stand-off distance

* *Corresponding author.*
E-mail: wangbingfeng@csu.edu.cn (B. Wang).
http://dx.doi.org/10.1016/j.jmrt.2016.04.001

[4–9]. Yang and Wang [10] described the structural changes in the melting zones as the vortex structure during the explosive cladding of titanium to mild steel. The vortex zones composed of amorphous and nanograins are easy to fracture during deformation. Honarpisheh and Asemabadi [11] investigated the formation of brittle intermetallic compounds in the melting zones. The intermetallic compounds exhaust the ductility and increase the risk of brittle fracture of the deformed metal [12–16]. The quality of the bonds and the melting zones strongly depends on careful control of the cladding parameters including the explosive load, the detonation velocity, the stand-off distance, the load ratio and/or collision angle. The selection of parameters is often based upon the mechanical properties, density and shear wave velocity of each component [1,17–19]. We often use the weldability windows to determine the possible values of the cladding parameters for the explosive cladding [2,4]. However, the relation between the thickness of the melting zone and the processing parameters of the explosive cladding is yet not clear.

The aims of this paper are (1) to investigate the thickness and morphology of the melting zones in the interface of the Ti/NiCr explosive cladding bar, and (2) to propose a physical model of the thickness of the melting zone, and (3) to discuss the effects of the cladding parameters on the thickness of the melting zone.

2. Method

The chemical composition and properties of the pure Ti and NiCr alloy used in the present work are given in Table 1. Commercial purity titanium (CP-Ti) tube was used as the clad material, and NiCr alloy bar was used as the base material. The surfaces of the base and clad materials were used as received. The emulsified explosive with the detonation velocity 3500–4000 m/s and the density 0.8–1.0 g/cm^3 was chosen as explosive material. The cylindrical arrangement was used for experimental set-up for explosive cladding as described elsewhere [15,16]. The explosive was uniformly placed around the tube. Selected parameters for explosive cladding bars were listed in Table 2.

Samples for optical microscope observations were cut in the cross-section of the cladding bar and normal to the plane of the cladding interface. The etchant for Ti side is 4 ml HNO_3 + 6 ml HCl + 5 ml HF + 100 ml H_2O, and the NiCr alloy side is not etched. Investigations of optical microscopy were performed with POLYVAR-MET. And then, the thickness of the melting zone was measured on the cross-section interface of the Ti/NiCr explosive cladding bar. We specify the radian interval (about 7 degrees) for measuring the thickness of the melting zone in the interface of the Ti/NiCr explosive cladding bar.

3. Results and discussion

3.1. *Thickness and morphology of the melting zones*

The Ti/NiCr explosive cladding bars were fabricated as shown in Fig. 1. Due to the inhomogeneous distribution of the explosive, the surfaces of the samples were slightly burned.

Fig. 1 – (a) Picture of the Ti/NiCr explosive cladding bars, (b) the corresponding cross-section images.

Fig. 2 shows the morphology of the interface of the explosive cladding bar. It can be seen that boundaries of the melting zones are nearly circular arcs, whose center points to the center of the NiCr bar.

Cross-sections optical microscope of the cladding bar is given in Fig. 3. Local melting zones are encountered in sections of the cladding interface. Lots of Bamboo-shaped cracks can also be found in the melting zones. The amorphous and the intermetallic compounds exhaust the ductility and increase the risk of brittle fracture of deformed metal. The bamboo-shaped cracks are formed in the melting zone [15,16].

Fig. 4 shows the thickness and distributions of the melting zones in the cross-sections of the Ti/NiCr explosive cladding

Table 1 – The chemical composition of the materials (wt%).

Elements	C	Si	N	S	Ti	Cr	Fe	Ni
NiCr	0.08	1.38	–	0.12	–	21.27	0.37	76.78
CP-Ti	0.08	0.02	0.03	–	99.57	–	0.30	–

Table 2 – The cladding parameters and the corresponding thickness of the melting zones.

Sample	Load ratio (R)	Base bar diameter (R/mm)	Stand-off distance (S/mm)	Explosive thickness (δ_f/mm)	Thickness of the melting zone (δ_m/mm)
No. 1	2.48	7	5	20	0.2773
No. 2	4.22	13	2	34	0.2360
No. 3	2.48	13	2	20	0.1377
No. 4	1.99	13	2	16	0.1728
No. 5	1.24	13	2	10	0.1237
No. 6	1.24	10	1	10	0.0696
No. 7	1.24	7	0.5	10	0.0356

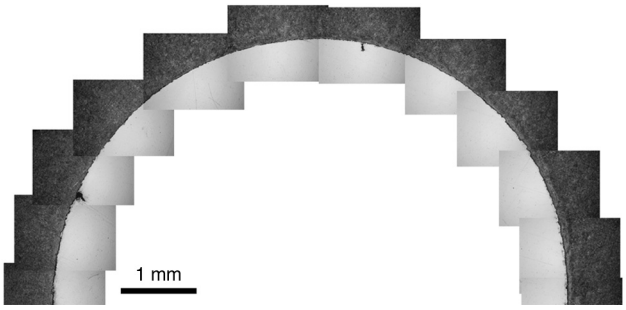

Fig. 2 – Interfacial morphology of the Ti/NiCr explosive cladding bar (sample No. 7).

bar (sample No. 3). The average thickness of the melting zones is about 0.1377 mm. Table 2 illustrates the average thickness of the melting zones vs. the cladding parameters in all samples. It can be seen that the average thickness of melting zones decreases with reducing of the stand-off distance or the thickness of the explosive.

3.2. *Physical model of the melting zone*

We assume that the material is homogeneous and incompressible, and the effect of air in the flyer tube movement and the influence of lateral rarefaction wave can be ignored, and circumferential stress in the flyer tube movement are negligible, and the stress on the materials are homogeneously distributed.

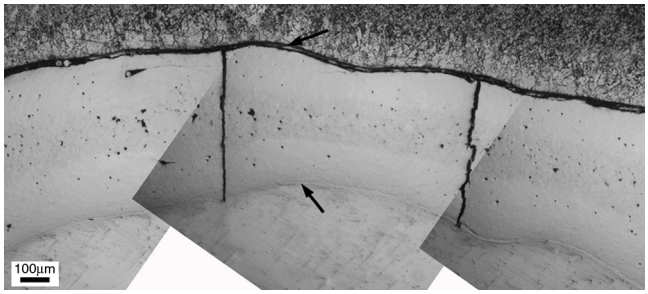

Fig. 3 – The typical morphology of the melting zone.

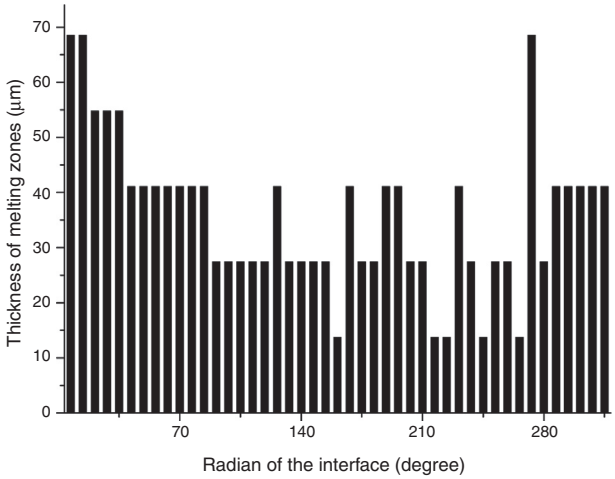

Fig. 4 – Spectra of the distribution of the measured thickness of the melting zone in the interface of the Ti/NiCr explosive cladding bar (sample No. 7).

After flyer pipe collided to the base bar, the kinetic energy of flyer pipe (E) converts into various forms of energy, including bonding energy (E_1), plastic deformation energy (E_2), vibration energy (E_3), crater energy (E_4), sound energy (E_5) and the kinetic energy of sand or gravel (E_6). The kinetic energy of flyer pipe (E) and the energy conversion can be described as follows.

$$E = \frac{1}{2}MV_p^2 \tag{1}$$

$$E = E_1 + E_2 + E_3 + E_4 + E_5 + E_6 \tag{2}$$

where V_p is the impact velocity, M is the weight of the unit area of the flyer metal. The bonding energy (E_1) induces the melting of materials in the interface. That is, part of the kinetic energy converted into melting heat energy leading to the formation of the melting zone. Thus,

$$\frac{1}{2}MV_p^2 k_0 = CM_0\Delta T \tag{3}$$

$$M_0 = \rho\delta_m \tag{4}$$

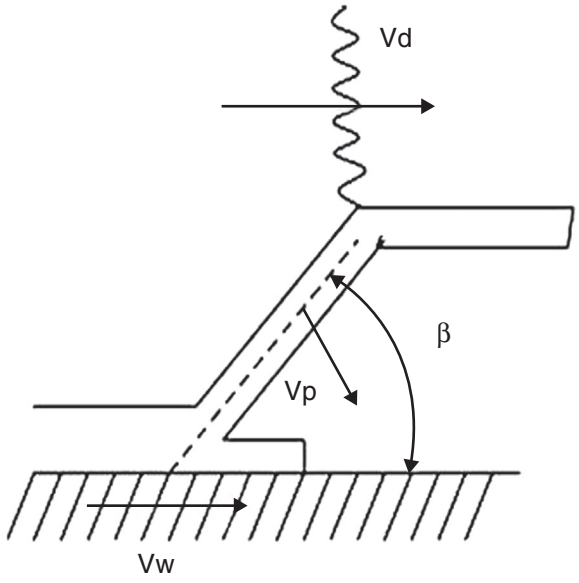

Fig. 5 – Schematic of the explosive cladding process.

where k_0 is a conversion coefficient between kinetic energy and heat energy; C, M_0, ΔT, δ_m and ρ are specific heat of the melting zone, the weight per area, temperature rise, the thickness and the density of the melting zone, respectively.

For explosive cladding technique, the cladding parameters can be summarized as follows: the impact velocity (V_p), the collision point velocity (V_w), the dynamic angle of collision (β), the explosive detonation velocity (V_d), the thickness of explosive (δ_f), and stand-off distance (S). As the detonation is initiated, the flyer metal (plate or pipe) is drastically accelerated by the pressure of detonation and flies with high velocity toward the base metal (plate or pipe), as shown in Fig. 5. The stand-off distance provides the distance across which the flyer metal can be accelerated and reached the necessary impact velocity for the formation of metallurgical bonding between flyer metal and the base metal [20]. Thus, the bonding process can be described as follows.

$$P(t)S = \frac{1}{2}M(V_p^2 - V_0^2) \tag{5}$$

The stand-off distance (S) can be obtained by the following equation.

$$S = \frac{M(V_p^2 - V_0^2)}{2P(t)} \tag{6}$$

where $P(t)$ and V_0 are the pressure on the flyer metal and the initial velocity of the flyer metal, respectively. The flyer metal reaches a velocity at the moment of the detonation and flies toward the base metal at this velocity [21,22]. The initial velocity of the flyer metal can be obtained as follows.

$$V_0 = 2V_d \sin\left(\frac{\beta}{2}\right) \tag{7}$$

where V_d is explosive detonation velocity. The appropriate value of the dynamic angle of collision (β) is often as $5^\circ < \beta < 25^\circ$ [8]. The jet between the cladding materials cannot generate until β is above β_c [7]. The following equation gives the critical value of the dynamic angle of collision (β_c).

$$\beta_c = k_1\sqrt{\frac{HV}{\rho_1 V_d^2}} \tag{8}$$

where β_c is in radians, k_1 is a constant, and HV is the Vickers hardness. k_1 is determined by the conditions of the cladding materials' surface. The values of k_1 for high-quality pre-cleaning of surfaces and imperfectly cleaned surfaces are 0.6 and 1.2, respectively. Generally, the value of k_1 is 0.85 [22].

The pressure on the flyer metal is given by [22]:

$$P(t) = \frac{\rho_0 V_d^2}{1+\gamma} e^{\left\{-\left[\frac{bR+c}{(1+\gamma)\delta_f}\right]t\sqrt{V_d^2+U^2}\right\}} \tag{9}$$

where b and c are constants, ρ_0, R, γ, δ_f and t are the density of explosive, load ratio, polytropic exponent, the thickness of the explosive, and the time, respectively. Generally, $\gamma = 3$ [22].

At the beginning of the explosive detonation, the pressure on the flyer metal reaches to the maximum value P_{max}, as follows.

$$P_{max} = \frac{\rho_0 V_d^2}{(1+\gamma)} \tag{10}$$

The pressure on the flyer metal reduces gradually during the explosive cladding. Thus, the average pressure (P_a) on the flyer metal can be obtained as follows.

$$P_a = \frac{P_{max}}{2} = \frac{\rho_0 V_d^2}{2(1+\gamma)} \tag{11}$$

Substituting Eqs. (5), (7) and (11) into Eqs. (3) and (4), the thickness of melting zone (δ_m) is obtained as follows.

$$\delta_m = \frac{k_0(\rho_0 V_d^2 S + 16\rho_1\delta_e V_d^2 \sin^2(\beta/2))}{8C\rho\Delta T} \tag{12}$$

where $\rho_1\delta_e$ is given as follows [23].

$$\rho_1\delta_e = 0.1\left(\frac{\rho_0\delta_f}{k_2}\right)^2 \tag{13}$$

where k_2 is a constant, and in the general case, $k_2 = 1.5$ [23].

And then,

$$\delta_m = k_0\left(\frac{K_{E1}}{K_M}S + \frac{32}{45}\frac{K_{E2}}{K_M}\delta_f^2\right) \tag{14}$$

where K_{E1} and K_{E2} are constants of the explosive, K_M is constant of materials.

$$K_{E1} = \rho_0 V_d^2 \tag{15}$$

$$K_{E2} = \left(\sin\frac{\beta}{2}\right)^2 \rho_0^2 V_d^2 \tag{16}$$

$$K_M = 8C\rho\Delta T \tag{17}$$

Table 3 – Comparison of measured and calculated thickness of melting zone.

Samples	No. 1	No. 2	No. 3	No. 4	No. 5	No.6	No. 7
Measured thickness (mm)	0.2773	0.2360	0.1377	0.1728	0.1237	0.0696	0.0356
Calculated thickness (mm)	0.2856	0.2826	0.1548	0.1304	0.1041	0.0605	0.0387
Relative error	2.9%	19.7%	12.5%	24.5%	13.4%	13.1%	8.7%

Table 4 – List of symbols.

List of symbols	
V_p	Impact velocity
M	Weight of the unit area of the flyer metal
k_0	Conversion coefficient
C	Specific heat of the melting zone
M_0	Weight of the unit area of the melting zone
ΔT	Temperature rise
V_w	Collision point velocity
β	Dynamic angle of collision
V_d	Explosive detonation velocity
S	Stand-off distance
$P(t)$	Pressure on the flyer metal
V_0	The initial velocity of the flyer metal
ρ_0	Density of explosive
R	Load ratio
γ	Polytropic exponent
δ_f	Thickness of explosive
t	Time
δ_e	Thickness of flyer metal
β_c	Critical value of the dynamic angle of collision
k_1	Constant
HV	Vickers hardness
P_a	Average pressure
δ_m	Thickness of the melting zone
ρ	Density of the melting zone
k_2	Constant
M_1	Volume fraction of the titanium
M_2	Volume fraction of the nickel
M_3	Volume fraction of the chromium
C_1	Specific heat of the titanium
C_2	Specific heat of the nickel
C_3	Specific heat of the chromium
ρ_1	Density of the flyer metal (pure titanium)
ρ_2	Density of the nickel
ρ_3	Density of the chromium

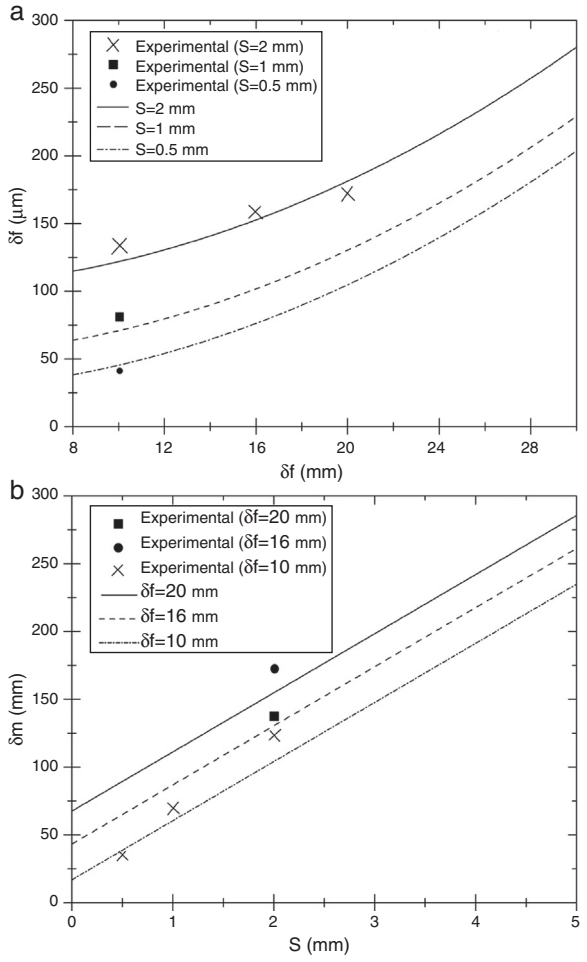

Fig. 6 – (a) The thickness of the melting zone as a function of the thickness of the explosive for different stand-off. (b) The thickness of the melting zone as a function of the stand-off for different thickness of the explosive.

3.3. *Effects of the cladding parameters*

The melting zone formed in the cross-section of the Ti/NiCr explosive cladding bar is composed of 32 at% titanium (M_1), 51 at% nickel (M_2) and 17 at% chromium (M_3) [15]. The specific heat (C) and the density (ρ) of the melting zone can be estimated from the specific heat and the density of the pure metals weighted by the volume fraction of each element, as follows.

$$C = \frac{C_1M_1 + C_2M_2 + C_3M_3}{M_1 + M_2 + M_3} \tag{18}$$

$$\rho = 0.25\rho_1 + 0.55\rho_2 + 0.2\rho_3 \tag{19}$$

where C_1, C_2 and C_3 are specific heat capacity of pure titanium, nickel and chromium, respectively; ρ_1, ρ_2 and ρ_3 are the density of pure titanium, nickel and chromium, respectively. $C_1 = 527.4\,J/kg^\circ C$, $C_2 = 460\,J/kg^\circ C$, $C_3 = 450\,J/kg^\circ C$, $\rho_1 = 4510\,kg/m^3$, $\rho_2 = 8902\,kg/m^3$, and $\rho_3 = 7190\,kg/m^3$. Besides, $\Delta T = 3507\,K$ [16] and $\beta = 8^\circ$. Substituting the above parameters into Eqs. (14)–(19), the thickness of the melting zone can be obtained as follows.

$$\delta_m = 0.2114k_0S + 0.8182k_0\delta_f^2 \tag{20}$$

The cladding parameters and the corresponding average thickness of the melting zones are given in Table 2. We employed the six specimens (Nos. 1–6) for fitting the parameters of Eq. (14). The value of k_0 is 0.206. Thus,

$$\delta_m = 0.0436S + 0.169\delta_f^2 \tag{21}$$

For sample No. 7, the measured thickness of the melting zone is 35.6 microns, and the predicted thickness calculated by Eq. (21) is about 38.7 microns. The relative error $\Delta = (\left|(\delta_{m\,\exp} - \delta_m)/\delta_{m\,\exp}\right| \times 100\%)$ is 8.7%. We compared the measured thickness with the calculated thickness of the melting zones, as illustrated in Table 3. Therefore, the physical model of the melting zone can be used to predict the thickness of the melting zone in the interface of Ti/NiCr explosive cladding bar (Table 4).

The values of the thickness of the melting zone for Ti/NiCr explosive cladding bar can be obtained by integrating the parameters into Eq. (21) as shown in Fig. 6. In Fig. 6a, the stand-off distance is varied from 0.5 mm to 2 mm. In Fig. 6b, the thickness of explosive (δ_f) is varied from 10 mm to 20 mm. The result indicates that values of thickness of the melting zones (δ_m) increase with increasing of the stand-off distance (S) and the thickness of explosive (δ_f), as shown in Fig. 6a and b, respectively.

4. Conclusions

The distribution of the local melting zone in the interface of the Ti/NiCr explosive cladding bar is uniform and axisymmetric, and boundaries of the melting zone are circular arcs, whose center points to the center of the NiCr bar. The bamboo-shaped cracks generate in the melting zone. The thickness of the melting zone decreases regularly with reducing of the stand-off distance and the thickness of explosive. The thickness of the melting zone in the interface of the explosive cladding bar can be described as a function of the stand-off distance and the thickness of explosive.

Conflicts of interest

The authors declare no conflicts of interest.

Acknowledgments

This work was financial supported by Hunan Provincial Natural Science Foundation of China (No. 12JJ2028), and by a scholarship from the China Scholarship Council (No. 201308430093), and by the Freedom Explore Program of Central South University (No. 2015zzts175), and by State Key Laboratory of Powder Metallurgy, Central South University.

REFERENCES

[1] Blazynski TZ. Explosive welding, forming and compaction. London: Applied Science Publishers; 1983.
[2] Findik F. Recent developments in explosive welding. Mater Des 2011;32:1081–93.
[3] Kacar R, Acarer M. An investigation on the explosive cladding of 316L stainless steel-din-P355GH steel. J Mater Process Tech 2004;152:91–6.
[4] Mousavi SAAA, Sartangi PF. Experimental investigation of explosive welding of cp-titanium/AISI 304 stainless steel. Mater Des 2009;30:459–68.
[5] Durgutlu A, Gulenc B, Findik F. Examination of copper/stainless steel joints formed by explosive welding. Mater Des 2005;26:497–507.
[6] Acarer M, Demir B. An investigation of mechanical and metallurgical properties of explosive welded aluminum–dual phase steel. Mater Lett 2008;62:4158–60.
[7] Zamani E, Liaghat GH. Explosive welding of stainless steel–carbon steel coaxial pipes. J Mater Sci 2012;47:685–95.
[8] Kahraman N, Gulenc B, Findik F. Joining of titanium/stainless steel by explosive welding and effect on interface. J Mater Process Tech 2005;169:127–33.
[9] Han JH, Ahn JP, Shin MC. Effect of interlayer thickness on shear deformation behavior of AA5083 aluminum alloy/SS41 steel plates manufactured by explosive welding. J Mater Sci 2003;38:13–8.
[10] Yang Y, Wang BF, Xiong J. Amorphous and nanograins in the bonding zone of explosive cladding. J Mater Sci 2006;41:3501–5.
[11] Honarpisheh M, Asemabadi M, Sedighi M. Investigation of annealing treatment on the interfacial properties of explosive-welded Al/Cu/Al multilayer. Mater Des 2012;37:122–7.
[12] Gulenc B. Investigation of interface properties and weldability of aluminum and copper plates by explosive welding method. Mater Des 2008;29:275–8.
[13] Wronka B. Testing of explosive welding and welded joints. Wavy character of the process and joint quality. Int J Impact Eng 2011;38:309–13.
[14] Bataev IA, Bataev AA, Mali VI, Pavliukova DV. Structural and mechanical properties of metallic–intermetallic laminate composites produced by explosive welding and annealing. Mater Des 2012;35:225–34.
[15] Wang BF, Chen W, Li J, Liu ZL, Zhu XB. Microstructure and formation of melting zone in the interface of Ti/NiCr explosive cladding bar. Mater Des 2013;47:74–9.
[16] Wang BF, Luo XZ, Wang B, Zhao ST, Xie FY. Microstructure and its formation mechanism in the interface of Ti/NiCr explosive cladding bar. J Mater Eng Perform 2015;24:1050–8.
[17] Mousavi SAAA, Al-Hassani STS. Numerical and experimental studies of the mechanism of the wavy interface formations in explosive/impact welding. J Mech Phys Sol 2005;53:2501–28.
[18] Mousavi SAAA, Al-Hassani STS, Burley SJ. Simulation of explosive welding using the Williamsburg equation of state to model low detonation velocity explosives. Int J Impact Eng 2005;31:719–34.
[19] Crossland B. Explosive welding of metals and its applications. Oxford: Clarendon Press; 1982.
[20] Raghukandan K. Analysis of the explosive cladding of Cu–low carbon steel plates. J Mater Proc Tech 2003;139:573–7.
[21] Grignon F, Benson D, Vecchio KS, Meyers MA. Explosive welding of aluminum to aluminum: analysis, computations and experiments. Int J Impact Eng 2004;30:1333–51.
[22] Shao BH, Zhang K. Basic principal of explosive welding and its engineering application. Dalian: Dalian Science and Technology University Press; 1987.
[23] Dalian shipyard research group. Explosive cladding. Dalian: Chinese Journal of Theoretical and Applied Mechanic; 1977.